

# Accurate Tropospheric Correction for Local GPS Monitoring Networks With Large Height Differences

Steffen Schön, Andreas Wieser, and Klaus Macheiner  
*Engineering Geodesy and Measurement Systems (EGMS)*  
*Graz University of Technology*

## BIOGRAPHY

Dr. Steffen Schön studied geodesy at University Karlsruhe (Germany) and IGN (Paris, France). In 2003, he received the degree of Dr.-Ing. from University Karlsruhe. His main research topics at University Karlsruhe and the German Geodetic Research Institute (DGFI, Munich) have been the analysis and optimization of geodetic measurement procedures (especially high precision GPS) with respect to systematic effects. At EGMS he has been involved in several GPS projects, especially on landslide monitoring. Currently, he is a Feodor-Lynen post-doctoral fellow at EGMS working on GPS correlation.

Dr. Andreas Wieser has worked as a University Assistant with the Department of Engineering Geodesy and Measurement Systems (EGMS) at the Graz University of Technology since 1998. He has been involved in various research areas related to parameter estimation, high precision GPS applications, quality control, fuzzy logic, and metrology in civil engineering. From 2003 to 2004 he has been a post-doctoral fellow with the Department of Geomatics Engineering at the University of Calgary, since 2004 he is with EGMS again.

Klaus Macheiner received the degrees Bakk. techn. (Geomatics Engineering) and Dipl.-Ing. (Geomatics Science) from the Graz University of Technology in 2003 and 2004, respectively. During the last months he has been involved in several projects concerning precise surveying and GPS at EGMS. Currently, he is a University Assistant at this institute.

## ABSTRACT

Tropospheric induced distortions of point coordinates are still a major error source when using GPS for high precision geodetic monitoring applications. Using data from a local GPS landslide monitoring network (height

differences up to 900 m), we found that the apparent height variations caused by residual tropospheric propagation effects can reach up to 6 cm if only a priori tropospheric models are applied. This is an order of magnitude worse than the required accuracy of better than 0.5 cm. It can be shown that the apparent height variations in each monitoring station depend linearly on the height difference with respect to the stable reference station. This proportionality is the key and the starting point for the development of the correction models.

We discuss two approaches to mitigate such errors, one in the observation domain and one in the coordinate domain. Both approaches exploit the height dependence of the relative tropospheric delay among stations subject to the same atmospheric conditions. The results show that both approaches reduce most of the bias of the height component, e.g., typical long periodic distortions of up to 6 cm during 3 hours are reduced to less than 1cm. This is a reduction of over 80%.

## INTRODUCTION

In engineering geodesy, local network configurations with large height differences are very common, e.g., for the GPS monitoring of landslides or the deformation analysis of large structures like e.g., bridges and towers. The analysis of these GPS networks shows that the height component is impaired by residual tropospheric effects if only a priori tropospheric models are applied like e.g., the Saastamoinen (1973) model, cf. e.g., Gurtner (1989), Brunner et al. (2003).

For post processing applications, various correction strategies have been developed for small networks with large height differences. Gurtner et al. (1989) and Beutler et al. (1995) compare three approaches for the Turtmann network with height differences up to 1500 m. The three approaches are (i) the estimation of station specific tropospheric parameters, (ii) the use of actual ground meteorological

logical data, and (iii) the estimation of height proportional tropospheric group delays. All three approaches perform well for the analyzed network.

For real time monitoring using GPS, it is a challenge to separate tropospheric induced apparent height variations from actual antenna motions. The above approaches were originally developed for use with static applications and may not be readily applicable to kinematic positioning because of the high correlation between tropospheric delay and height estimate. An effective reduction of the apparent network distortion can be achieved also in kinematic applications when including at least one additional stable station besides the reference station, cf. Rührmöbl et al. (1998). This station is then used as a *calibration station* to permanently adjust the tropospheric correction model to the prevailing atmospheric conditions. This idea can be exploited in the coordinate domain or in the observation domain.

This approach differs from those proposed in the context of network RTK since no network of reference stations is processed and only two stable stations are needed. For an overview on network RTK correction techniques refer to e.g., Lachapelle and Alves (2002) and references therein.

The correction in the coordinate domain is quite straight forward. During the network adjustment the coordinates of the calibration station are processed like those of the monitoring stations. Its apparent height variations are attributed to residual tropospheric effects. They are scaled and subtracted from the estimated heights of the monitoring stations. The scaling factor depends only on a known ratio of height differences between the network stations.

A more flexible alternative is the correction model in the observation domain, which needs to be implemented in the adjustment model or Kalman filter. Here, in addition to the coordinates a tropospheric coefficient is set up as a stochastic process and estimated from all observations. The height component of the calibration station is fixed or heavily constrained, so this station mostly contributes to the estimation of the tropospheric coefficient.

The basic assumption for both approaches is that all GPS stations (monitoring stations as well as the reference and the calibration station) are subject to the same atmospheric conditions. This holds usually for stations located on the same slope. If this assumption is not justified, the approaches can easily be extended to treat the stations as groups and apply an individual correction model to each of the groups e.g., for points on different sides of an Alpine ridge, cf. Gurtner et al. (1989).

In the next section of this paper, the GPS landslide monitoring network at Gradenbach in Austria is described. This network will be used subsequently to demonstrate

the tropospheric delay correction. Then, the correction model in the coordinate domain is developed and applied to two representative 24h data sets. The following section is devoted to the correction model in the observation domain. It turns out that both models effectively and efficiently reduce the residual tropospheric variations in the height component. Finally, the advantages of both models are discussed and compared to a stochastic modeling of station specific tropospheric parameters.

## DESCRIPTION OF THE GPS LANDSLIDE MONITORING GRADENBACH

Since 1999, the Institute of Engineering Geodesy and Measurement Systems (EGMS) at Graz University of Technology has carried out continuous GPS monitoring of the Gradenbach landslide in the summer months (May to October), cf. Brunner et al. (2003). This deep-seated mass movement is situated in the central Austrian Alps. The active deformation zone, covering an area of about 2 km<sup>2</sup>, involves the entire slope with widths ranging from 600 to 1000 m. Vertically, the slide extends over approximately 1000 m in height from the slide toe (between 1100 and 1270m) to the head scarp (2270 m) lying slightly below the mountain ridge. This area is represented in yellow in Fig. 1.

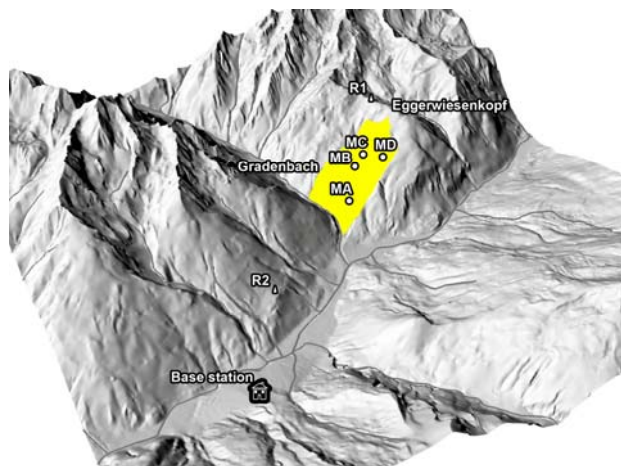


Fig. 1: Situation of the Gradenbach landslide.

Fig. 1 shows a digital terrain model of the Gradenbach area (5x5 km<sup>2</sup>) and the location of the 6 GPS stations (2 stations R1 and R2 in stable bedrock, and 4 monitoring stations MA, MB, MC, and MD on the slope) as well as the base station for data storage and online processing. All 6 GPS station are equipped with Ashtech G12 or Ashtech UX L1/L2 receivers, and Ashtech choke-ring antennas with SCIS-type radome. The total equipment is lightning protected. For the registration a data rate of 3 sec and a cut-off angle of 5° were chosen. The data transmission to the base station is realized by radio link.

In addition to the online-processing in the Kalman filter-based software GRAZIA (Gassner et al., 2002), twice per year - at the beginning and end of the campaign - a 48h static reference solution is computed using the BERNESE GPS software (5.0). For a documentation of BERNESE 5.0 see Hugentobler et al. (2004). For this network solution a sampling rate of 30 sec and a cut-off angle of  $10^\circ$  as well as elevation dependent variances of the observations are used. The baselines are built with respect to the stable station R2 (*reference station*) cf. Fig. 1. The mathematical correlations are properly modeled. Precise IGS products such as precise orbits and the global ionosphere model are introduced. Further, NGS relative antenna phase center variations and offsets are applied (Mader, 1999). The coordinates of the reference station are fixed during the network adjustment. Tab. 1 lists the baseline lengths and height differences with respect to the reference station. The ambiguities are fixed according to the strategy proposed by Hugentobler et al. (2004). Finally, tropospheric parameters are estimated for all stations except the reference station with a temporal resolution of 2h.

Tab. 1: Gradenbach GPS monitoring network: Comparison of baseline lengths and height differences with respect to the reference station R2.

station name	baseline lengths [km]	ellipsoidal height differences [km]
MA	2.6	0.0
MB	3.2	0.3
MC	3.5	0.4
MD	3.5	0.5
R1	4.6	0.9

## CORRECTION MODEL IN THE COORDINATE DOMAIN

### Mathematical formulation

Most of the tropospheric delay can be taken into account by applying a correction model like e.g. the Saastamoinen (1973) model. However, even when using highly accurate meteorological measurements instead of a standard atmosphere model, and even when including a sophisticated mapping function, there will always be a residual tropospheric error of the double differenced observations. Gurtner et al. (1989) have shown that this residual tropospheric delay distorts the heights for GPS networks with large height differences, while the horizontal coordinate components are hardly affected. In addition, they have stated that the height distortions are proportional to the height values. If all stations are submitted to the same atmospheric conditions, the proportionality factor is identical for the whole network. This condition is met for GPS landslide monitoring where all stations are located on the same slope or at least in the same valley.

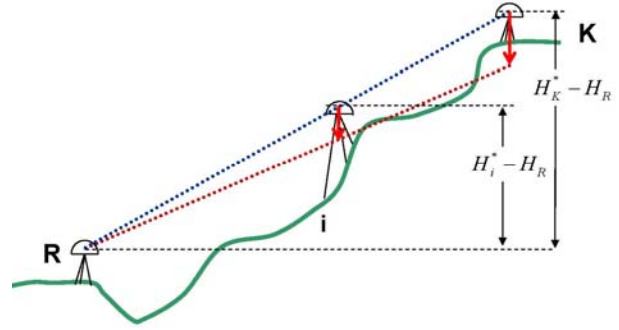


Fig. 2: Principle of the correction model in the coordinate domain.

Fig. 2 shows the principle of the correction model in the coordinate domain. In blue the ‘true’ (error-free) heights are represented. The red dashed line shows the height-dependent scaling of the network due to residual tropospheric effects. The apparent height variations are depicted by red arrows at the calibration station K and the monitoring station  $i$ .

The ‘true’ (error-free) heights  $H^*(t_r)$  at a reference epoch  $t_r$  and the estimated heights  $\hat{H}(t)$  at epoch  $t$  are related by

$$\hat{H}(t) = H^*(t_r) + \Delta H^*(t_r, t) + \sum \delta_i(t), \quad (1)$$

where  $\delta_i(t)$  denotes systematic effects caused by e.g., the troposphere, the ionosphere or multipath. The ‘true’ height difference between epoch  $t$  and the reference epoch is  $\Delta H^*(t_r, t)$ .

In the following we focus exclusively on tropospheric effects. Applying the correction model in the coordinate domain, the corrected height  $\hat{H}'_i(t)$  for the monitoring station  $i$  at epoch  $t$  and the corrected height differences  $\Delta \hat{H}'_i(t_r, t)$  between two epochs or with respect to the reference epoch  $t_r$  are given by

$$\hat{H}'_i(t) = \hat{H}_i(t) - f(\hat{H}_K(t) - H_K^*), \quad (2)$$

$$\Delta \hat{H}'_i(t_r, t) = \hat{H}_i(t) - \hat{H}_i(t_r) - f(\hat{H}_K(t) - \hat{H}_K(t_r)), \quad (3)$$

with the correction factor  $f$

$$f = \frac{H_i^* - H_R}{H_K^* - H_R}, \quad (4)$$

where

$\hat{H}_i(t)$ ,  $\hat{H}_i(t_r)$  denote the estimated heights of the monitoring station  $i$  at epoch  $t$  and the reference epoch  $t_r$ ,

$\hat{H}_K(t)$ ,  $\hat{H}_K(t_r)$  the estimated heights of the calibration station at epoch  $t$  and the reference epoch  $t_r$ ,

$H_i^*, H_K^*$  the ‘true’ heights of the monitoring station  $i$ , and the calibration station  $K$  at the reference epoch  
 $H_R$  the ellipsoidal height of the reference station.  
 The solution at the reference epoch may be a single epoch solution as well as a static solution.

The correction by Eq.(2) depends on the ‘true’ height of the calibration station. For a correction better 0.5 mm, the heights in the correction factor (Eq.(4)) should be known better than 1 m. Since the differences between the processed heights and their ‘true’ values are generally smaller than 1m, these values in Eq.(4) can be replaced by the processed values and Eq.(3) is independent of any ‘true’ heights. Considering only tropospheric effects  $\delta_{Trop}$ , Eq.(3) can be rewritten as

$$\Delta \hat{H}_i'(t_r, t) = \Delta H_i^*(t_r, t) + \Delta \delta_{Trop, i}(t_r, t) - f \Delta \delta_{Trop, K}(t_r, t) \quad (5)$$

$$\approx \Delta H_i^*(t_r, t)$$

where no actual motion occurs for the stable calibration station.

For the quality of the correction the following aspects play a role:

- (i) The heights of the calibration station and the reference station should be upper and lower bounds to the heights of all monitoring stations. This avoids extrapolation, and the height dependent correction factor (Eq.(4)) is then always smaller than 1.

For the Gradenbach network, this factor varies between 0 (no correction) for the station MA located on the same height as the reference station R2 (cf. Tab. 1) and 0.5 for the station MD.

- (ii) In Eqs.(2) and (3) the apparent height deviations at the calibration station are attributed exclusively to residual tropospheric effects  $\delta_{Trop}$ .

Therefore, station specific effects such as multipath might be transferred from the calibration station to the monitoring stations if they are not properly mitigated. For this task, the raw height time series of the calibration station could be filtered previous to the correction step to remove short periodical fluctuations caused by multipath. The use of proper observation weight models and a sound quality control strategy should be mandatory, anyway.

- (iii) Due to satellite obstruction e.g., by trees or mountain ridges, different satellites may be visible at the calibration and the monitoring stations, yielding some geometric effects in the correction. Strictly, the correction should only be applied if only satellites tracked at all stations were considered when processing the raw GPS observations. However, such a rejection of available

information may weaken the geometry of the coordinate solution significantly, and may therefore annihilate any accuracy gain possibly achieved by the correction model. Therefore, we do not recommend using only common satellites. Eqs.(2) to (5) are still a useful correction model.

### Numerical example

Two representative 24h L1 data sets (D1: 10/15/2003 00:00-24:00 UT, D2: 05/27/2004 00:00-24:00 UT) were chosen for the comparison of the correction models. The processing was carried out in MATLAB with an extended Kalman filter, cf. Gelb (2001) or Brown and Hwang (1997). For this processing, IGS precise orbits, Klobuchar-style ionospheric model coefficients supplied by the University of Berne (CODE), and relative antenna phase center offsets and variations from NGS were used. The Saastamoinen (1973) model was applied as an a priori tropospheric model. The coordinates of the BERNESE (5.0) static reference solution (10/14/2003 16:00 UT-10/16/2003, 10:00 UT) served as initial coordinates for the dynamic solution of both datasets by the Kalman-filter based software.

A sampling rate for the dynamic processing of 30 sec and a cut-off angle of  $10^\circ$  were chosen. The observations were weighted according to the SIGMA- $\epsilon$  variance model (Hartinger and Brunner, 1999)

$$\sigma^2 = C \cdot 10^{\frac{-C/N_0}{10}} \quad (6)$$

with some constant  $C$  depending on the used GPS equipment. Using the  $C/N_0$ -values of the observations, this model allows to reduce the impact of signal distortion effects.

The North, East and height coordinate errors are modeled as independent random walk processes. Taking into account the maximum annual displacements detected so far (0.5 m), the spectral noise densities were introduced as

$$q = \frac{(\frac{1}{3} 0.5)^2 \text{ m}^2}{365.5 \cdot 24 \cdot 3600 \text{ s}} = 8.8 \cdot 10^{-10} \text{ m}^2 \text{ Hz} \cdot \quad (7)$$

The a priori standard deviation of all station coordinates except those of the reference station (fixed) was set to  $\sigma_{y,0} = 1 \text{ cm}$ , hence the variance-covariance matrix of the initial state reads

$$\mathbf{P}_0^{(+)} = \sigma_{y,0}^2 \mathbf{I} \cdot \quad (8)$$

### Raw coordinate time series

Fig. 3 shows the resulting raw coordinate time series for the 24h L1 data set D1. The variations with respect to the BERNESE static reference solution for the five stations MA, MB, MC, MD and R1 are depicted in mm.

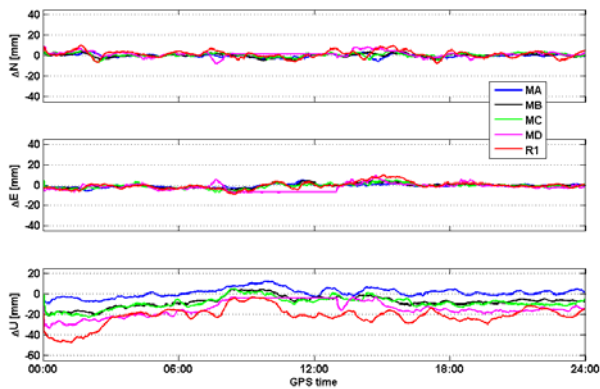


Fig. 3: Data set D1 (October 2003): Resulting raw coordinate time series for the East, North and Up component with respect to the BERNESE reference solution of October 2003.

The horizontal coordinate components vary about 0, i.e., the BERNESE reference solution, with maximum amplitudes of 5 mm. This is expected since the data set D1 is a subset of the data used for the BERNESE solution. During these 24h no actual motion occurred. Therefore, the jitter of the time series reflects the impact of observation noise, station specific effects, residual ionospheric effects and residual tropospheric effects. Peaks in the time series are associated with periods of weak geometry and individual ambiguity resolution problems. A data gap occurred between 08:21 and 12:59 at the station MD, so the filter output is constant during this period (prediction only), see Fig. 3.

The height components show additional systematic offsets with a typical height dependent distortion pattern. This implies that (i) the height component with the largest height differences are distorted most (here R1), cf. Fig. 5. (ii) The height component of stations with the same ellipsoidal height as the reference station should not be affected, cf. MA in Fig. 5.

This pattern is due to the fact that only an a priori tropospheric model (Saastamoinen) is applied during the processing of the data set while tropospheric parameters were estimated with a temporal solution of 2h for the reference solution. Obviously, this a priori model cannot eliminate the total tropospheric propagation effect. An apparent height dependent residual effect remains in the time series. The mean magnitude of the offset indicates the disagreement of the actual meteorological conditions and those intrinsically presumed by the a priori tropospheric model.

In Fig. 4, the resulting raw coordinate time series are plotted for the second selected 24h L1 dataset (D2). The reference for the computation of coordinate differences is again the same reference solution as above (i.e., of October 2003).

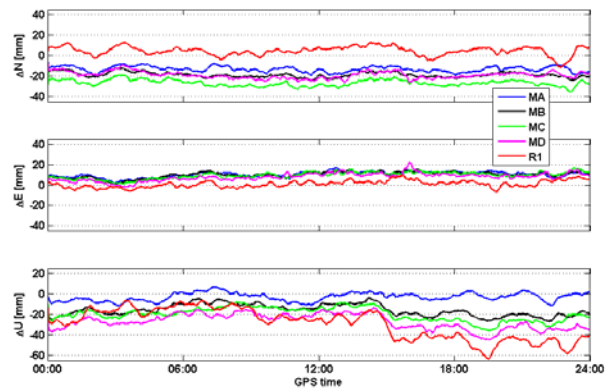


Fig. 4: Data set D2 (May 2004): Resulting raw coordinate time series with respect to the BERNESE reference solution of October 2003.

Since an actual point displacement occurred between October 2003 and May 2004, the coordinate differences vary no longer about 0. The average long-term point displacements of this landslide are

$$\frac{\Delta N}{\Delta t} = -4 \frac{\text{cm}}{\text{year}}, \quad \frac{\Delta E}{\Delta t} = 2 \frac{\text{cm}}{\text{year}}, \quad \frac{\Delta U}{\Delta t} = -3 \frac{\text{cm}}{\text{year}}, \quad (9)$$

This means that we may expect offsets of about  $-2$  cm,  $1$  cm, and  $-1.5$  cm for the North, East, and height component, respectively. Station R1 does not move, because this station is located in stable bedrock above the mass movements, cf. Fig. 1. This stability was confirmed by an analysis of the variation of the coordinate differences between R2 and R1 during the past 5 years.

We see from Fig. 4 that the displacements computed from the GPS data agree well with the above values except for the height component. The actual height displacement is superimposed on the apparent motion caused by residual propagation effects. For the detailed analysis it helps to study the time series of the stable point R1 first, and to consider two time periods: 00:00–15:00 and 15:00–24:00. During the first period, the apparent motion is small ( $-2$  cm), i.e., the atmospheric conditions are similar to those intrinsically assumed by the a priori tropospheric model. Therefore, the height dependent distortion pattern is not clearly pronounced and superimposed by the actual point displacement, e.g., the station MD shows the largest height deviation.

This situation is completely different for the second period ( $\sim 15:00-24:00$ ). Due to a thunderstorm with rainfall and a sudden drop in temperature ( $10$  °C), the atmospheric conditions change completely, which was verified by official meteorological data. These changes are directly reflected by the increase of the apparent height variations, i.e., in a strong disagreement between actual meteorological conditions and those assumed by the a priori tropospheric model. The height dependent distortion pattern is now very well pronounced and feigns significant height variations. It can be seen that for this sec-

ond period the height dependent pattern includes - besides the height dependent biases - similar signatures at all stations with height proportional amplitudes, cf. Fig. 5 (bottom).

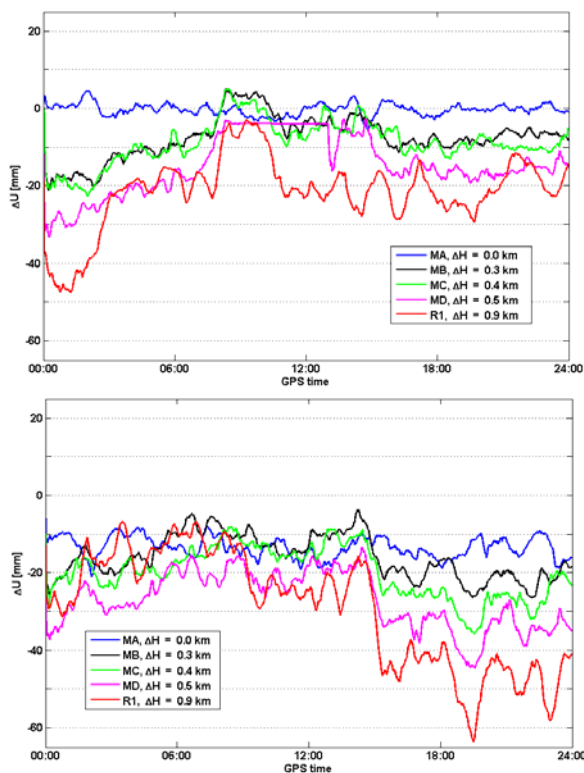


Fig. 5: Comparison of the resulting raw height variations with respect to the BERNESE reference solution of October 2003. Top: October 2003 bottom May 2004. The height difference to the reference station R2 is indicated by  $\Delta H$ .

### Corrected time series

In the second step, these raw coordinate time series are corrected applying the correction model (Eq.(3)), where the stable point R1 serves as the calibration station.

Fig. 6 shows the corrected height time series for both data sets when applying the correction model in the coordinate domain. Only the height component is depicted since this correction model does not affect the other coordinate components. Their values equal the raw time series, depicted in figures 4 and 5. The corrected time series for October 2003 vary about 0 with amplitudes of less than 1cm.

The corrected time series for May 2004 show remaining offsets at all stations except at the stable calibration station R1. They indicate the magnitude of the actual station displacements between October 2003 and May 2004, which are roughly about -1.5cm in height. This agrees

well with the long-term velocity discussed above, cf. Eq.(9). Again the scattering of the corrected time series is less than 1cm. It is especially interesting to see that the correction model handles extremely quickly the changing atmospheric conditions during the session D2.

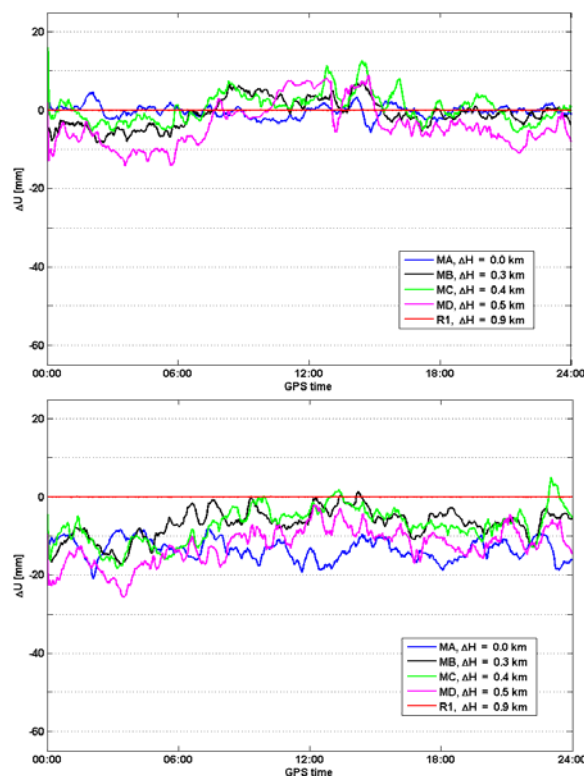


Fig. 6: Comparison of the corrected height time series of all stations for the data set D1 (top) and D2 (bottom) after application of the correction model in the coordinate domain.

Once the heights have been corrected using the above equation, one can extract the ‘true’ motion of the monitoring points between October 2003 and May 2004 from the resulting time series, cf. Eq.(5).

### CORRECTION MODEL IN THE OBSERVATION DOMAIN

#### Mathematical formulation

A different realization of the same basic idea is a correction model in the observation domain. This approach is based on a post processing algorithm initially proposed by the Bernese GPS group, cf. e.g., Gurtner et al. (1989). The total tropospheric delay  $T_i^j(t)$  is formulated in the following way

$$T_i^j(t) = m f_i^j(t) \left( T_i^{j,0}(t) + \sum_{l=0}^m \mu_l(t) (H_i^* - H_R)^l \right), \quad (10)$$

where  $mf_i^j(t)$  denotes the mapping function,  $T_i^{j,0}(t)$  the tropospheric zenith delay given by an a priori tropospheric model, e.g., the Saastamoinen model (1973), and  $H_i^*$  is the ‘true’ heights in [km] of the station  $i$  and  $H_R$  the ellipsoidal height of the reference station. Since the height difference in Eq. (10) is only needed with an accuracy of some decimeters the actual height  $\hat{H}_i^{(+)}$  processed by the Kalman filter can be used. The tropospheric coefficients  $\mu_i(t)$  are estimated as parameters.

If all stations are submitted to the same atmospheric conditions and the network is small, only the first order coefficient  $\mu_i(t)$  needs to be considered. In this case Eq.(10) reads

$$T_i^j(t) = mf_i^j(t) \left( T_i^{j,0}(t) + \mu(t) (H_i^0 - H_R) \right). \quad (11)$$

The constant offset  $\mu_0$  is not observable in a small network and cancels effectively when processing double differences. However, the second order term in Eq.(10) may have to be retained if the height differences in the monitoring network are larger than 1000 m, cf. Beutler et al. (1995, p.120f). For the real-time application, the first order coefficient  $\mu_i(t)$  is set up as additional stochastic process and therefore as state in the Kalman filter.

Based on the hypothesis of identical meteorological conditions, principally all double differences contribute to the estimation of the tropospheric coefficient, cf. Eq.(11). Three aspects are important for the determination of their individual impact. (i) Regarding Eq.(11) it is obvious that observations at low elevations have a larger contribution to the estimation of the tropospheric coefficient than observations at high elevations. (ii) The larger the height difference with respect to the reference station the greater the impact of the observations of this station to the determination of the tropospheric coefficient, cf. Eq.(11). (iii) Finally, the ratio of the spectral noise densities of the tropospheric coefficient and the considered station coordinates determines which amount of information in the observations of this station are used for the estimation of the coordinates and which amount for the estimation of the tropospheric factor. If the coordinates of one station are e.g., fixed, all information is used for the estimation of the tropospheric coefficient.

For the quality of the correction the following recommendations should be considered. (i) Similar to the approach in the coordinate domain it is important to reduce signal diffraction by proper variance models (e.g. Hartinger and Brunner (1999), Brunner et al. (1999), or Wieser (2002)), and to apply a sound quality test strategy, see e.g., Wieser et al., (2004). (ii) In order to separate actual and apparent motion, the monitoring points should be processed together with some stable stations which are not submitted to the actual motion. The number of these calibration sta-

tions depends on their height differences with respect to the reference station, their process noise, and the magnitude and dynamics of the actual motion. For a slow mass movement like the Gradenbach landslide one constrained calibration station with large height differences (R1) is sufficient.

### Numerical example

The stochastic process of the tropospheric coefficient needs to be defined. The a priori value is set to  $\mu(t_0) = 0$ .

We have found that  $\sigma_{\mu,0} = 10^{-2} \text{ m/km}$  is a reasonable standard deviation for an alpine network of the Gradenbach type. We have further assumed a random walk process for this coefficient with a spectral noise density of  $q_\mu = 3.08 \cdot 10^{-9} \text{ m}^2/\text{km}^2 \cdot \text{Hz}$ . This value corresponds to changes of  $1 \text{ cm/km}$  during 3 h and was obtained from numerical simulations using typical diurnal variation of temperature, pressure and humidity in alpine regions.

The calibration station R1 is now set up as random walk as well (like the monitoring stations). The spectral noise density and the initial standard deviation are selected such as to heavily constrain this station as compared to the monitoring stations. We have chosen  $q_{cal} = 8.8 \cdot 10^{-14} \text{ m}^2/\text{Hz}$  and  $\sigma_{0,cal} = 0.1 \text{ mm}$  for all three components.

### Corrected time series

The following figures show the coordinate time series of the data sets D1 and D2 as obtained using the correction model in the observation domain. This model affects all coordinate components – although it has only little effect on the North and East components.

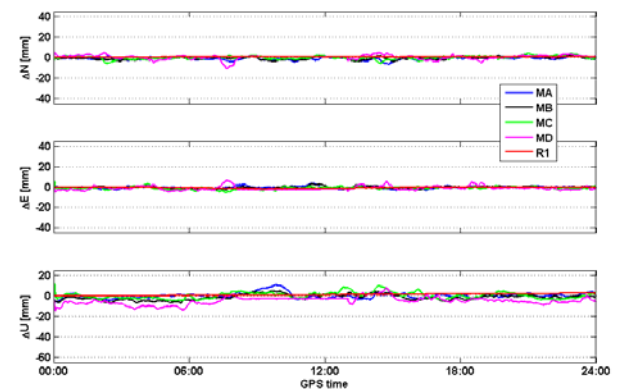


Fig. 7: Data set D1 (October 2003): Corrected coordinate time series of all stations after application of the correction model in the observation domain.

Fig. 7 shows the results for the data set D1 (October 2003) for the five stations MA, MB, MC, MD and R1.

The coordinate variations with respect to the BERNESE reference solution (October 2003) are given. The horizontal components vary about 0 with maximum amplitudes of 1 cm. Here only very small differences between the raw data (Fig. 3) and the corrected time series can be distinguished. This is quite obvious since the residual tropospheric delay affects mainly the height component. The time series for the horizontal components of R1 are very smooth and close to 0. This is due to the chosen a priori coordinate standard deviation and the low spectral noise density. In fact this choice allows to treat R1 as a calibration station, i.e., most of its apparent height motion is considered as being troposphericly induced.

The apparent motion in the height component is corrected for all stations. The corrected time series vary about 0, i.e., the reference solution of BERNESE. The maximum remaining amplitudes are smaller than 1 cm.

Fig. 8 shows the corrected time series for the data set D2 (May 2005) with respect to the BERNESE static reference solution of October 2003. The corrected time series clearly show the actual point displacement between October 2003 and May 2004, i.e., a displacement of 2 cm to 3 cm in South, 1 cm in East and 1.5 cm in height. This direction corresponds to the maximum gradient of the slope. Again the time series of R1 are very smooth because this station is used as calibration station. Its values are close to 0 since the calibration station does not move.

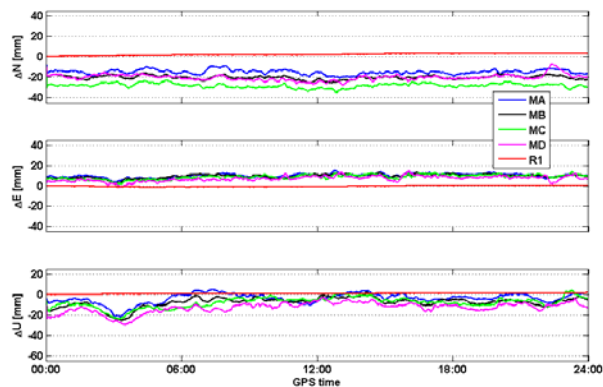


Fig. 8: Data set D2 (May 2004): Corrected coordinate time series of all stations for the data set with the application of the correction model in the observation domain.

Comparing Fig. 5 and Fig. 9 it can be seen that the correction model in the observation domain is also suitable to correct the apparent height motion induced by residual tropospheric effects for different data sets and varying atmospheric conditions. The results compare well to those obtained by the correction in the coordinate domain (cf. Fig. 6) when averaged over the 24h interval. However the separation of movement and troposphere by the correction model in the observation domain is only possible if the dynamics of the troposphere and that one of the mass

movement are different. This is the case for slow mass movements like the Gradenbach landslide.

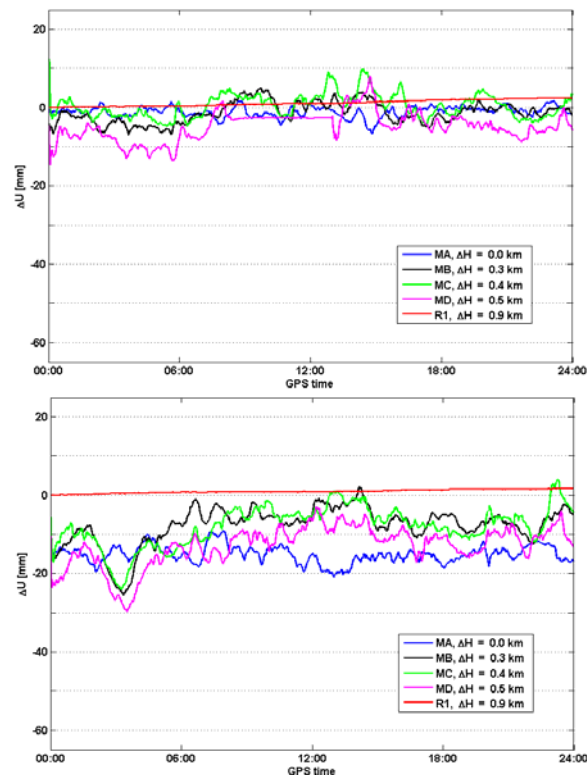


Fig. 9: Comparison of the resulting height variations after application of the correction model in the observation domain. Top: October 2003, bottom: May 2004. The variations are given with respect to the BERNESE reference solution of October 2003. The height difference to the reference station R2 is indicated by  $\Delta H$ .

## COMPARISON WITH STATION SPECIFIC TROPOSPHERIC PARAMETERS

Comparing the results of the previous sections, it can be stated that both models perform very well for the different atmospheric conditions in the data sets D1 and D2. The major part of the troposphericly induced height distortion reaching values up to 6 cm is reduced by more than 80%. Further, these approaches allow to separate apparent and actual point motions with respect to the reference solution, cf. Eq.(3) and (5) and the results in Fig. 6 and Fig. 9 for data set D2. These actual motions are of interest for geodetic deformation analysis (Caspary, 1988). If no actual motion occurs, the repeatability of the network solutions at consecutive epochs is improved. Nevertheless it is worth to investigate and to compare the stochastic modeling of station specific tropospheric parameters in the Kalman filter. This approach yields corrected heights without the need of stable calibration stations.

For this task, the initial processing strategies for the generation of the raw time series are changed in the following way. A stochastic process for the station specific relative tropospheric parameters  $\tau_i(t)$  is set up for all stations except the reference station. Then the total tropospheric correction reads

$$T_i^j(t) = mf_i^j(t)(T_i^{j,0}(t) + \tau_i(t)), \quad (12)$$

where  $mf_i^j(t)$  denotes the mapping function and  $T_i^{j,0}(t)$  the tropospheric zenith delay given by an a priori tropospheric model, e.g., the Saastamoinen model (1973).

According to Tralli and Lichten (1990) the tropospheric parameters can be equivalently modeled by a first order Gauss-Markov process or a random walk process. For the random walk process they reported spectral noise densities of

$$q_\tau = 6.25 \cdot 10^{-8} \dots 9 \cdot 10^{-8} \text{ m}^2 \text{ Hz}. \quad (13)$$

Here, we chose a random walk process with spectral noise density of

$$q_\tau = 6.2 \cdot 10^{-8} \text{ m}^2 \text{ Hz}, \quad (14)$$

However, we found that the results for the present data sets are not very sensitive to this value. Its a priori variance is chosen as  $\sigma_\tau^2 = 0.01 \text{ m}^2$  and the a priori value as  $\tau_{i,0} = 0 \text{ m}$ . The random processes of all station specific tropospheric parameters are supposed to be uncorrelated. Since this approach does not need any calibration station, the station R1 is treated like a monitoring station, cf. Eq.(7).

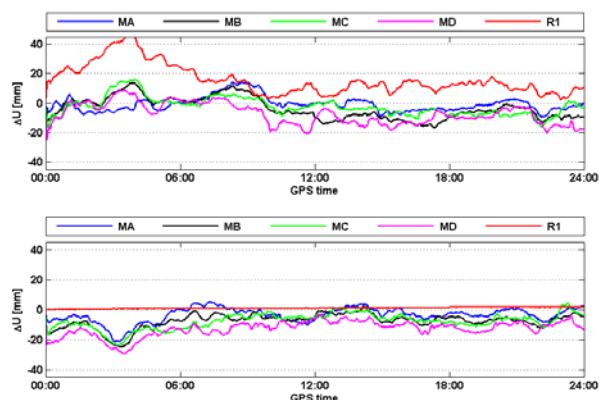


Fig. 10: Data set D2 (May 2004): Comparison of the resulting height variations after set up of station specific tropospheric parameters (top) and application of the correction model in the observation domain (bottom). The variations are given with respect to the BERNESE reference solution of October 2003.

Fig. 9 shows a comparison of the resulting corrected time series for the data set D2 by the stochastic modeling of station specific tropospheric parameters (Eq.(12)) and by the correction model in the observation domain, cf. Eq.(11).

Of course, stochastic modeling of station specific tropospheric parameters can reduce the impact of residual tropospheric effects to a certain amount, too. However, the main challenge of this approach is the separation of tropospheric parameter and station height. Therefore the height component shows large variations which are larger than those of the initial time series, cf. Tab. 2 third and fourth column. In addition, this approach is less suitable to separate actual and apparent height movement, especially in highly kinematic situations. The above models involving a calibration station mitigate this problem by computing the tropospheric correction mostly from the calibration station data which are not affected by antenna motion.

Tab. 2: Standard deviations [mm] of the height differences (30s time series) computed with and without correction models.

Data set	Station	Prior model only	Site specific stochastic modelling	Correction in the coordinate domain	Correction in the obs. domain
D1	MA	4.3	5.0	4.3	2.7
	MB	5.6	5.9	3.6	2.7
	MC	5.6	6.2	3.7	3.0
	MD	7.6	9.1	5.6	3.6
	R1	7.3	7.9	---	(0.8)
D2	MA	4.1	5.1	4.1	5.0
	MB	5.6	7.4	3.8	5.0
	MC	6.5	6.3	4.5	5.1
	MD	7.3	7.2	4.6	5.1
	R1	14.8	10.4	---	(0.4)

Tab. 2 indicates the variations of the time series in terms of standard deviations for data set D1 and D2. Tab. 3 gives the reduction of these variations by the different correction models. We start analyzing the results for the data set D1. For the raw height time series, the standard deviations increase with the height difference due to the height proportional biases. The time series after estimation of station specific tropospheric parameters shows an even larger variability as the raw time series, cf. Tab. 3 second column. This is due to the fact that the height component and the tropospheric parameter are difficult to separate and the resulting heights are therefore very unstable. Finally, the correction in the coordinate domain as well as in the observation domain, reduces the variability, and standard deviations of less than 5 mm can be obtained for the 30-second coordinate time series. For the correction in the coordinate domain, a reduction of the standard deviation of about 30% is obtained. The correction in the observation domain performs even better, cf. Tab. 3.

Hence the application requirements for height precision applications are met.

Tab. 3: Reduction of standard deviations [%] by different correction models.

Data set	Station	Site specific stochastic modelling	Correction in the coordinate domain	Correction in the obs. domain
D1	MA	16	0	-37
	MB	6	-35	-51
	MC	10	-34	-47
	MD	19	-27	-53
D2	MA	23	0	21
	MB	32	-31	-12
	MC	-4	-31	-21
	MD	-1	-37	-30

For the data set D2 the raw height time series shows a similar variability except station R1. Here the large standard deviation reflects the dramatic changes in the atmospheric conditions during this 24h data set. Again the estimation of station specific tropospheric parameters is not able to reduce this variability, cf. Tab. 3 (second column). For the correction model in the observation and coordinate domain, similar standard deviations as above are obtained, despite the significant change of atmospheric conditions which occurred, see above. Again, a reduction of 30% in the standard deviation is obtained by the correction model in the coordinate domain for the stations MB, MC, and MD.

## CONCLUSIONS

In this paper two different correction models for height distortions, which are caused by residual tropospheric delays, are discussed: a correction in the coordinate domain and a correction model in the observation domain implemented in the Kalman filter. The basic idea for an effective reduction is the inclusion of at least one additional stable station in bedrock, beside the reference station. This station is then used as a *calibration station* to permanently adjust the tropospheric correction model to the prevailing atmospheric conditions, cf. Rührnößl et al. (1998). After the application of the correction models the resulting time series of height differences between consecutive epochs or with respect to common reference epoch are largely free of apparent height variations induced by residual tropospheric delays.

Using the example of the Gradenbach landslide it was shown that for GPS deformation monitoring in a network with large height differences (here up to 900 m with distances of less than 5 km) residual tropospheric effects can cause height errors of several cm. Both models are suit-

able to mitigate these effects and obtain 30-second height time series with a standard deviation of about 5 mm. Higher precision is obtainable with lower temporal resolution. This contributes to a better separation between actual and tropospheric induced apparent station displacements. Consequently, if no actual station displacement occurs, the repeatability of the height component is improved.

The approach in the coordinate domain is attractive because it is computationally extremely efficient and applicable in real time as well as in post processing. In addition it can be applied externally to the coordinate output of any commercial GPS processing software or time series already available. However, there are limitations, mainly the impact of station specific effects at the calibration station and of different satellite geometry at different sites of the network.

The implementation in the observation domain, directly in the Kalman filter is extremely flexible, and the impact of the calibration station can be tuned by selecting the properties of the stochastic process modeling its coordinates. Furthermore, the estimated coefficient is more robust against distorted observations at the calibration station, because all network stations contribute to the estimated tropospheric correction.

For both models, a specific network geometry is preferable, in which the heights of the reference station and the calibration station are lower and upper bounds of the monitoring stations. In addition, an adequate quality control of the observations and an appropriate weight model should be used.

## ACKNOWLEDGMENTS

The continuous GPS monitoring of the Gradenbach landslide is supported by the Austrian Academy of Sciences in the framework of an ISDR project. Rainer Klostius is acknowledged for providing the BERNESE (5.0) reference solutions. He and Fritz Zobl are acknowledged for providing figure 1. The Alexander von Humboldt-Foundation is gratefully acknowledged for the financial support of the first author. The basic idea of using a *calibration station* was proposed and developed in the coordinate domain by Fritz K Brunner. He is acknowledged for many fruitful discussions and his input on this topic.

## REFERENCES

Beutler G, Geiger A, Rothacher M, Schaer S, Schneider D, Wiget A (1995) Dreidimensionales Testnetz Turtmann 1985-1993, Part 2 (GPS-Netz) Geodätische-geophysikalische Arbeiten in der Schweiz. Vol.51 Swiss Geodetic Commission, Zurich, Switzerland

Brown R, Hwang P (1997) Introduction to random signals and Kalman filtering 3<sup>rd</sup> ed. Wiley and Sons, New York

Brunner FK, Zobl F, Gassner G (2003) On the Capability of GPS for Landslide Monitoring. *Felsbau* 21(2): 51-54

Brunner FK, Hartinger H, Troyer L (1999) GPS signal diffraction modelling: the stochastic SIGMA- $\Delta$  model, *Journal of Geodesy*, 73:259-267

Caspary W (1988) Concepts of network and deformation analysis. 2d impression, Monograph 11 School of surveying, The University of New South Wales, Kensington, Australia.

Gassner G, Wieser A, Brunner FK (2002): GPS Software Development for Monitoring of Landslides. In: Proceedings of the XXII FIG Congress Washington TS6.4.

Gelb A (2001) Applied optimal estimation. 16 edition MIT Press Cambridge MA.

Gurtner W, Beutler G, Botton S, Rothacher M, Geiger A, Kahle H, Schneider D, Wiget A (1989) The use of the Global Positioning System in mountainous areas. *manuscripta geodaetica* 14:53-60

Hartinger H, Brunner FK (1999) Variances of GPS Phase Observations: The SIGMA- $\epsilon$  Model. *GPS Solution* 2/4:35-43.

Hugentobler U, Dach R, Fridez P (2004) Bernese GPS Software Version 5.0, Astronomical Institute University of Berne.

Lachapelle G, Alves P (2002) Multiple Reference Station Approach: Overview and Current Research. *Journal of Global Positioning Systems* 1(2): 13-136

Mader G (1999): GPS Antenna Calibration at the National Geodetic Survey. *GPS Solutions* 3(1):50-58

Rührnöbl H, Brunner FK, Rothacher M (1998) Modellierung der topospherischen Korrektur für Deformationsmessungen mit GPS im alpinen Raum. *Allgemeine Vermessungsnachrichten* 105(1):14-20

Saastamoinen J (1973) Contribution to the theory of atmospheric refraction. Part II refraction corrections in satellite geodesy. *Bulletin géodésique* 107:13-34

Tralli D, Lichten S (1990) Stochastic estimation of tropospheric path delays in Global Positioning System geodetic measurements. *Bulletin géodésique* 64:127-159

Wieser A (2002) Robust and fuzzy techniques for parameter estimation and quality assessment in GPS. Doc-

toral thesis, Graz University of Technology, Shaker Verlag, Germany

Wieser A, Petovello M, Lachapelle G (2004) Failure Scenario to be Considered with Kinematic High Precision Relative GNSS Positioning. *ION GNSS 2004* 1448-1459